

Probing the Single-Particle Character of Rotational States in ^{19}F Using a Short-Lived Isomeric Beam

D. Santiago-Gonzalez,^{1,2} K. Auranen,² M. L. Avila,² A. D. Ayangeakaa,^{2,*} B. B. Back,² S. Bottoni,^{2,†} M. P. Carpenter,² J. Chen,² C. M. Deibel,¹ A. A. Hood,¹ C. R. Hoffman,² R. V. F. Janssens,^{2,‡} C. L. Jiang,² B. P. Kay,² S. A. Kuvvin,³ A. Lauer,¹ J. P. Schiffer,² J. Sethi,^{4,2} R. Talwar,² I. Wiedenhöver,⁵ J. Winkelbauer,⁶ and S. Zhu²

¹Department of Physics and Astronomy, Louisiana State University, Baton Rouge, Louisiana 70803, USA

²Physics Division, Argonne National Laboratory, Argonne, Illinois 60439, USA

³Department of Physics, University of Connecticut, Storrs, Connecticut 06269, USA

⁴Department of Chemistry and Biochemistry, University of Maryland, College Park, Maryland 20742, USA

⁵Department of Physics, Florida State University, Tallahassee, Florida 32306, USA

⁶Los Alamos National Laboratory, Los Alamos, New Mexico 87544, USA



(Received 9 January 2018; published 23 March 2018)

A beam containing a substantial component of both the $J^\pi = 5^+$, $T_{1/2} = 162$ ns isomeric state of ^{18}F and its 1^+ , 109.77-min ground state is utilized to study members of the ground-state rotational band in ^{19}F through the neutron transfer reaction (d,p) in inverse kinematics. The resulting spectroscopic strengths confirm the single-particle nature of the $13/2^+$ band-terminating state. The agreement between shell-model calculations using an interaction constructed within the sd shell, and our experimental results reinforces the idea of a single-particle–collective duality in the descriptions of the structure of atomic nuclei.

DOI: [10.1103/PhysRevLett.120.122503](https://doi.org/10.1103/PhysRevLett.120.122503)

The duality of the collective and single-particle descriptions of the structure of atomic nuclei has been recognized for some 60 years. It is perhaps best summarized by an excerpt from the Nobel lecture of Aage Bohr [1,2], “It was quite a dramatic moment when it was realized that some of the spectra in the light nuclei that had been successfully analyzed by the shell-model approach could be given a very simple interpretation in terms of the rotational coupling scheme.” Central to these comments by Bohr was the “special role” played by the ^{19}F nucleus, one of the lightest nuclei to exhibit rotational features. At that time, the ^{19}F spectrum had just been described by both shell-model calculations assuming only a small number of valence nucleons [3,4], as well as by a collective model assuming rotational structures [5,6].

Since these pioneering calculations, a great deal of work has been done aiming to refine the theoretical description of ^{19}F [7–15], not the least of which involved identifying the similarities between wave functions generated from both approaches [16] and the recent accessibility of ^{19}F to *ab initio* calculations [17]. Within a collective description, the ground-state rotational band in ^{19}F exhibits the characteristic staggering or “signature splitting” of a $K = 1/2$ rotational structure [18] where a measured static quadrupole moment points toward prolate deformation, and the states are linked by relatively enhanced electric quadrupole transitions. The band proceeds from its bandhead, with a spin parity of $J_{\min}^\pi = 1/2^+$ to its terminating state $J_{\max}^\pi = 13/2^+$. This termination is evidence for the importance of

shell structure since this is the maximum spin that can be generated from three nucleons in the sd shell outside the ^{16}O core.

The nucleus ^{18}F has a $J^\pi = 5^+$ excited state that consists of two maximally aligned $0d_{5/2}$ nucleons outside the closed-shell ^{16}O core [19]. This level has a 162(7)-ns half-life [14], comparable to the flight time of an ion beam in the tens of MeV/u range over a few meters. By producing a beam of this isomer (^{18m}F) and bringing it to a target, states in ^{19}F of $J \geq 5/2$, including the $13/2^+$ terminating state, can be produced by the addition of yet another $0d_{5/2}$ neutron.

In this Letter, we report on the extraction of spectroscopic overlaps between initial states in ^{18m}F and final states in ^{19}F , including the terminating $13/2^+$ state of the $K = 1/2$ rotational band, via the single-neutron (d,p) transfer reaction. Combined with a simultaneous measurement of the (d,p) reaction with a ^{18}F beam in its $J^\pi = 1^+$ ground state (^{18g}F), whereby the lower-spin members of the band were populated, a determination of the single-particle character of the ^{19}F ground-state rotational band was obtained for the first time in a single experiment.

The experiment was performed at the ATLAS facility at Argonne National Laboratory and utilized the HELIOS spectrometer [20,21], a device designed for measuring transfer reactions in inverse kinematics. A radioactive beam of ^{18}F at an energy of 14 MeV/u was produced with an intensity of $\sim 5 \times 10^5$ pps via the in-flight technique [22,23]. The $^2\text{H}(^{17}\text{O}, ^{18}\text{F})n$ production reaction was used

with an ^{17}O primary beam (15 MeV/u) at a typical intensity of 60 pA. A cryogenically cooled deuterium-filled gas cell (~ 80 K and 1.4×10^5 Pa) provided the production target material. The resulting ^{18}F beam was comprised of ions in both ground and isomeric states. Previous experiments using ^{18m}F beams include those of Refs. [24–28]. In the present work, the $^{18m}\text{F}/^{18g}\text{F}$ ratio has been estimated to be 0.56(8) immediately after production and 0.11(2) after transport to the HELIOS experimental station (details on this estimation are given below).

HELIOS was configured for the observation of protons in coincidence with ^{19}F from single-neutron transfer reactions (d,p) on beams of both ^{18g}F and ^{18m}F . The solenoidal field was set to 2.85 T and deuterated polyethylene (CD_2) targets with a nominal thickness of $400 \mu\text{g}/\text{cm}^2$ were placed near the center of the field region. Upstream of the target location, an on-axis position-sensitive Si detector array was installed for proton detection. Protons were uniquely identified from their cyclotron periods after completing a single orbit from the target to the Si detector array. A fast-counting, segmented ionization chamber [29] centered around 0° was positioned downstream of the target for ^{19}F recoil detection. Coincidence events between protons and recoiling ions were determined by the relative time difference between the two detectors. Acceptance for proton-recoil events was possible up to ~ 5 MeV in excitation energy, covering all but the $11/2_1^+$ member in the ^{19}F ground-state rotational band. The acceptance also included proton center-of-mass angles $\theta_{\text{c.m.}}$ ranging from $\sim 10^\circ$ to 35° .

Levels in ^{19}F populated by reactions on the isomeric beam appear shifted by -1.07 MeV relative to ground-state reactions, hence, the ‘‘apparent’’ qualifier in the angle-integrated excitation spectrum of Fig. 1. The shift is primarily the result of the Q -value difference between $^{18m}\text{F}(d,p)$ ($Q = 9.328$ MeV) and $^{18g}\text{F}(d,p)$ ($Q = 8.207$ MeV). In addition, an ~ 50 -keV shift arises from differences in the kinematics between the two reactions. The Q -value resolution was 280-keV FWHM, driven primarily by the target thickness and the emittance of the secondary beam. The best fit to the data using known ^{19}F excitation energies [14] is shown in Fig. 1 by the solid gray line. Details on the peak assignment are discussed below.

Angle-integrated cross sections were determined from measured yields for all states identified in Fig. 1. For the levels that were populated strongly, relative differential cross sections, $d\sigma/d\Omega$, and angular distributions were also derived and are presented in Fig. 2. The center-of-mass angle $\theta_{\text{c.m.}}$ for each data point in Fig. 2 corresponds to the average angle covered by one set of position-sensitive Si detectors and has an uncertainty of $\lesssim 0.5^\circ$. The upper limits on yields were determined for weaker states by an increase of 5% to the best-fit χ^2 value to the apparent excitation spectrum (Fig. 1). The cross section for levels populated by the isomeric component of the beam were corrected for the $^{18m}\text{F}/^{18g}\text{F}$ beam ratio at the HELIOS target.

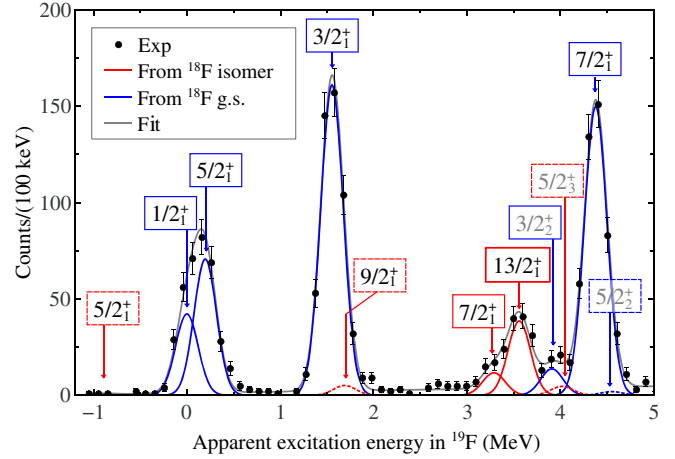


FIG. 1. Apparent excitation energy in ^{19}F extracted from protons in coincidence with ^{19}F recoils following $^{18g,m}\text{F}(d,p)$ reactions (black points with statistical uncertainties). A multi-Gaussian fit of the known levels in ^{19}F including a small linear background and fixed widths is shown in gray. States populated from (d,p) reactions on ^{18g}F are in blue, while those from ^{18m}F are in red. Weak levels, which, if removed from the fit would have little effect on the χ^2 value, are represented by dashed lines. Black labels identify states belonging to the ground-state rotational band.

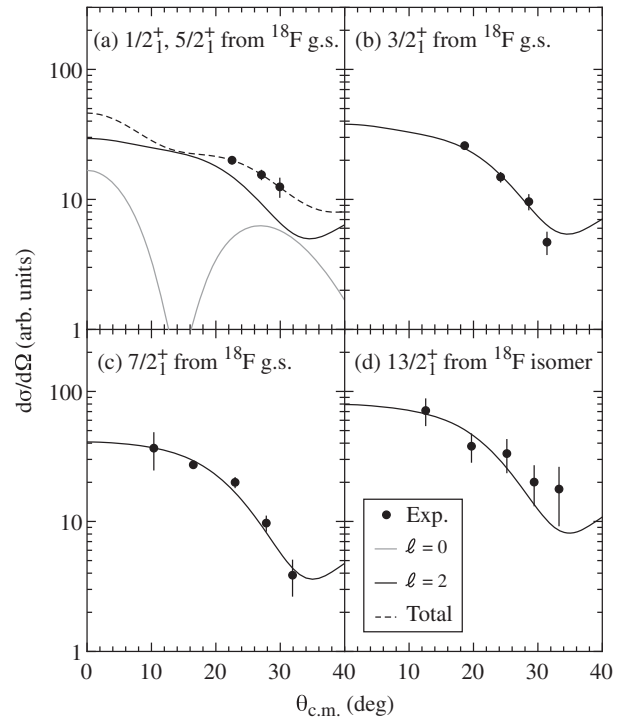


FIG. 2. Angular distributions for states in ^{19}F obtained from $^{18g}\text{F}(d,p)$ reactions, (a) $1/2_1^+$ and $5/2_1^+$ doublet, (b) $3/2_1^+$, (c) $7/2_1^+$, and from $^{18m}\text{F}(d,p)$ reactions, (d) $13/2_1^+$. The $13/2_1^+$ data include the 0.11(2) normalization factor to account for the $^{18m}\text{F}/^{18g}\text{F}$ secondary beam ratio. The DWBA calculations are represented by the lines.

The relative intensity of the isomeric 5^+ component of the ^{18}F beam compared to the 1^+ ground state was estimated by calculating the populations at the gas cell and then accounting for the reduction in the ratio over the flight time of the beam to the target at the HELIOS experimental station. There are no experimental data available for the (d,n) beam-production reaction at the relevant energies, and, therefore, the relative strengths of the population of the bound states of ^{18}F were taken from an analogous $^{17}\text{O}(^3\text{He},d)$ proton-transfer reaction [19]. The bulk of the relevant reaction yield proceeds to ten states below the proton separation energy in ^{18}F . The high-lying states decay by prompt γ -ray emission with known branching ratios to either ^{18}gF or $^{18\text{m}}\text{F}$ [14]. The $^2\text{H}(^{17}\text{O},^{18}\text{F})n$ cross sections were calculated with the distorted wave Born approximation (DWBA) utilizing the PTOLEMY code [30]. The DWBA prescription, including the choice of optical-model parameters, was validated through comparisons with available $^{16}\text{O}(d,p)$ cross-section data at a similar energy (13.15 MeV/u) [31].

The $^{18\text{m}}\text{F}/^{18\text{g}}\text{F}$ ratio at the production gas cell was calculated to be 0.56(8). The flight path from the gas cell to the HELIOS experimental station was 16.3 m, and at a beam energy of 14 MeV/u, it corresponds to a time of flight

of $1.9T_{1/2}$ of the isomeric state. Hence, the ratio at the HELIOS target was $^{18\text{m}}\text{F}/^{18\text{g}}\text{F} = 0.11(2)$.

The relative single-neutron overlaps (spectroscopic factors) between initial states in ^{18}F and final states in ^{19}F , S (isospin factor $C^2 = 1$) were extracted from the ratio of measured cross sections to those calculated with DWBA. In the standard procedure, the depth of the Woods-Saxon potential was varied to reproduce the binding energy of each final state. The deuteron wave function was calculated with the v_{18} potential [32]. A global set of optical-model parameters [33] was used to calculate the angular distributions shown in Fig. 2. Angular distributions obtained using a static set of parameters [34] produced similar results within uncertainties.

The S values resulting from the best fits of the DWBA calculations to the angular distributions (Fig. 2), as well as upper limits on the S values determined from the ratios of integrated cross sections, are given in Table I, while the spectroscopic strengths $(2J_i + 1)/(2J_f + 1)S$ are shown in Fig. 3. All S values have been normalized to the $3/2_1^+ - ^{18}\text{gF}$ transfer spectroscopic factor. Uncertainties on S are due to the choice of optical-model and bound-state parameters of the DWBA calculations. Uncertainty in the deduced $^{18\text{m}}\text{F}/^{18\text{g}}\text{F}$ ratio of the beam also contributes for levels which were populated by transfer on the isomer.

The data on the population of the ^{19}F $K = 1/2^+$ band are clearly present in the apparent excitation energy spectrum of Fig. 1. As expected from the relatively small isomeric component in our beam, the dominant features in our spectrum are similar to those in Fig. 2 of Ref. [35] and

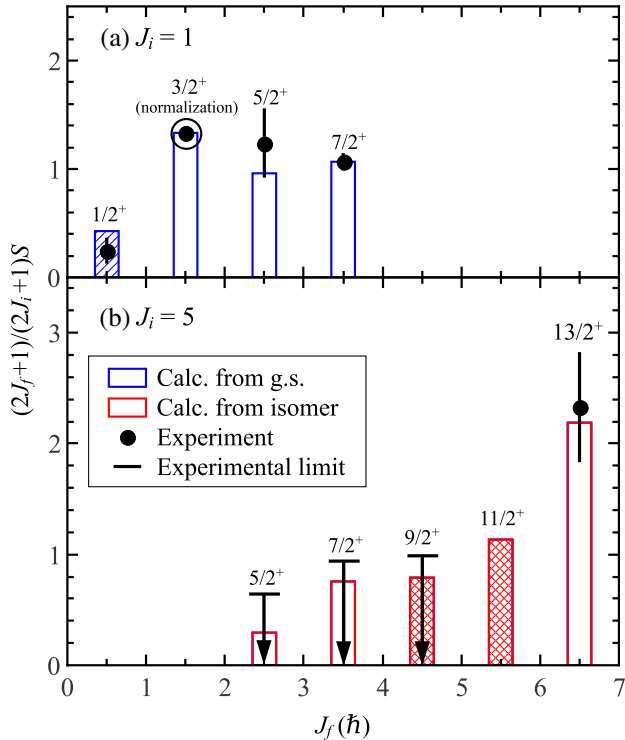


FIG. 3. The information on relative strengths of states in ^{19}F is plotted as a function of their spin separately for the $^{18}\text{gF}(d,p)$ (a) and $^{18\text{m}}\text{F}(d,p)$ reaction (b). The limit on the $9/2^+$ state is obtained assuming $\ell = 2$. Shell-model calculations using the USDB interaction are represented by bars for $\ell = 0$ (striped), 2 (open), or 0 and 2 (hatched) strengths.

TABLE I. Relative spectroscopic factors S for levels belonging to the ^{19}F $K = 1/2^+$ band [14]. All S values are normalized to that of the 1.554-MeV $3/2_1^+$ level. Only S values above 0.01 are shown and (\dots) signifies the nonobservation or inaccessibility of a given level.

E_f (MeV)	J_f^π	J_i^π	ℓ	S		
				Present	Ref. [35]	Theory ^a
0	$1/2_1^+$	1^+	0	0.4(2)	0.75(15)	0.64
0.197	$5/2_1^+$	1^+	2	0.6(2)	0.40(8)	0.48
		5^+	2	< 1.0 ^b	...	0.54
1.554	$3/2_1^+$	1^+	2	1	1	1
2.780	$9/2_1^+$	5^+	0	< 0.4 ^{b,c}	...	0.30
			2	< 1.2 ^{b,c}	...	0.57
4.378	$7/2_1^+$	1^+	2	0.40(3)	0.5(1)	0.39
		5^+	2	< 1.3 ^b	...	1.03
4.648	$13/2_1^+$	5^+	2	1.8(4) ^b	...	1.72
6.500	$11/2_1^+$	5^+	0	0.50
			2	0.54

^aShell-model calculations using the USDB interaction [15].

^bIncludes calculated value of 0.11(2) for the ^{18}F -isomer-to-g.s. ratio in the secondary beam.

^cAssumed pure ℓ transfer.

Fig. 5 of Ref. [36], where there was no isomeric component in the beam. The S values deduced for the lower-spin members of the $K = 1/2^+$ band populated by transfer on the ^{18}F , namely, the $1/2^+$ (0.000 MeV), $5/2^+$ (0.197 MeV), $3/2^+$ (1.554 MeV), and $7/2^+$ (4.378 MeV) ^{19}F states, are consistent with those from Ref. [35] (see Table I).

For the unresolved lowest-lying $1/2^+$ and $5/2^+$ levels, single line shapes with $\ell = 0$ and 2 transfers were assumed, respectively. Because of the limited angular coverage, our measurement is not sensitive to the population of the 0.110-MeV, $1/2^-$ level. The angular distributions of the $3/2^+$ and $7/2^+$ states did not require any sizable contributions ($> 5\%$) from $\ell = 0$ neutron transfer.

There are structures in the spectrum of Fig. 1 noticeable between 3 and 3.8 MeV, a featureless region in the ^{18}F transfer spectra of Refs [35,36]. Accounting for the -1.07 -MeV shift in apparent excitation energy for the (d,p) reaction on ^{18m}F , there are three previously known levels in this region that are accessible via $\ell = 0$ or 2 neutron transfer: the $7/2_1^+$ (4.378 MeV), $5/2_2^+$ (4.550 MeV), and $13/2_1^+$ (4.648 MeV) states [14]. Indeed, in the apparent energy spectrum of Fig. 1, lines corresponding to the population of the $13/2^+$ and $7/2^+$ levels are observed in the (3–3.8)-MeV range, identifying neutron transfer onto the isomeric 5^+ level of ^{18}F for the first time. Of the five other known levels also open to population through transfer on ^{18m}F in the energy region covered, upper limits on yields for the $5/2_1^+$ (-0.873 MeV), $9/2_1^+$ (1.710 MeV), and $5/2_3^+$ (4.037 MeV) states could be determined. The angular distribution for the $13/2^+$ state and the resulting DWBA fit [Fig. 2(d)] identify it as a strong $\ell = 2$ neutron transfer, solidifying its population from ^{18}F in its 5^+ isomeric state.

Accessibility to an in-flight beam of ^{18}F in both its ground 1^+ and fully stretched 5^+ states has enabled the extraction of (or setting limits on) the relative spectroscopic overlaps of the $1/2^+$, $3/2^+$, $5/2^+$, $7/2^+$, $9/2^+$, and $13/2^+$ members of the ground-state rotational band of ^{19}F (Table I and Fig. 3). The extracted S value for the $13/2^+$ state and its spectroscopic strength exceed those of all other states in the rotational band. This observation confirms the dominant single-particle configuration in this band-terminating state as corresponding to the maximally aligned state with a $\pi(0d_{5/2})^1_{j=5/2} \otimes \nu(0d_{5/2})^2_{j=4}$ configuration. This is the first direct measurement of the single-particle nature of a high-spin terminating state. This result together with the strengths of the levels populated from ^{18}F and the upper limits on the strengths of states populated from ^{18m}F describe the evolution of the single-particle strength of the states in the rotational band as a function of spin, from inception to termination (see Fig. 3).

Comparisons between the extracted S values and strengths of the present work to those calculated by the sd -confined USDB interaction [15] are also given in Table I and Fig. 3. The calculations are consistent with the experimental values, or limits, even though these

incorporate only three valence particles (one proton and two neutrons) and three active orbitals for each nucleon.

The present results highlight the single-particle character of the highest-spin state ($13/2^+$) in the rotational band of ^{19}F by confirming that the associated configuration corresponds to the maximally aligned, terminating state. Furthermore, we have found that the spectroscopic factors from shell-model calculations are consistent with our experimental values (and limits) for the ^{19}F states' members of the ground-state rotational band. Hence, some 40 years after his seminal statements [1,2], Bohr's dual interpretation of the ^{19}F sequence in terms of a collective and/or a single-particle excitation has been reinforced.

In summary, the single-particle character of members belonging to the ground-state rotational band in ^{19}F , including the terminating $13/2^+$ state, were probed in a single measurement via the (d,p) reaction. The relatively large spectroscopic strength observed for the $13/2^+$ level confirms the wave function purity expected in a maximally aligned, terminating state. Agreement between shell-model calculation and the experimentally determined spectroscopic factors for the inspected rotational states strengthens the notion of a collective and single-particle duality in the descriptions of the structure of atomic nuclei. The present measurement was possible only through the production of a beam of ^{18}F , whereby a significant fraction of ions resided in their short-lived isomeric state.

The authors thank C. Dickerson and R. C. Pardo for developing the ^{18}F isomeric beam. This material is based upon work supported by the U.S. Department of Energy, Office of Science, Office of Nuclear Physics, under Contract No. DE-AC02-06CH11357 (Argonne National Laboratory) and Grant No. DE-FG02-96ER40978 (Louisiana State University). This research used resources of Argonne National Laboratory's ATLAS facility, which is a Department of Energy Office of Science User Facility.

*Present address: Department of Physics, United States Naval Academy, Annapolis, Maryland 21402, USA.

†Present address: Università degli Studi di Milano and INFN sez. Milano, I-20133, Milano, Italy.

‡Present address: Department of Physics and Astronomy, University of North Carolina at Chapel Hill, Chapel Hill, North Carolina 27599-3255, and Triangle Universities Nuclear Laboratory, Duke University, Durham, North Carolina 27708-2308, USA.

- [1] A. Bohr, in *Physics 1971–1980*, edited by S. Lundqvist, Nobel Lectures (World Scientific, Singapore, 1992), p. 222, https://www.nobelprize.org/nobel_prizes/physics/laureates/1975/bohr-lecture.pdf.
- [2] A. Bohr, *Rev. Mod. Phys.* **48**, 365 (1976).
- [3] J. P. Elliott and B. H. Flowers, *Proc. R. Soc. A* **229**, 536 (1955).
- [4] M. Redlich, *Phys. Rev.* **99**, 1427 (1955).
- [5] E. B. Paul, *Philos. Mag.* **2**, 311 (1957).

- [6] G. Rakavy, *Nucl. Phys.* **4**, 375 (1957).
- [7] M. G. Redlich, *Phys. Rev.* **110**, 468 (1958).
- [8] A. Arima, S. Cohen, R. Lawson, and M. MacFarlane, *Nucl. Phys.* **A108**, 94 (1968).
- [9] I. Hamamoto and A. Atima, *Nucl. Phys.* **A112**, 481 (1968).
- [10] H. Benson and B. Flowers, *Nucl. Phys.* **A126**, 305 (1969).
- [11] M. Oyamada, T. Terasawa, K. Nakahara, Y. Endo, H. Saito, and E. Tanaka, *Phys. Rev. C* **11**, 1578 (1975).
- [12] B. A. Brown, B. H. Wildenthal, C. F. Williamson, F. N. Rad, S. Kowalski, H. Crannell, and J. T. O'Brien, *Phys. Rev. C* **32**, 1127 (1985).
- [13] B. Brown and B. Wildenthal, *Annu. Rev. Nucl. Part. Sci.* **38**, 29 (1988).
- [14] D. R. Tilley, H. R. Weller, C. M. Cheves, and R. M. Chasteler, *Nucl. Phys.* **A595**, 1 (1995).
- [15] B. A. Brown and W. A. Richter, *Phys. Rev. C* **74**, 034315 (2006).
- [16] J. P. Elliott, *Proc. R. Soc. A* **245**, 128 (1958).
- [17] S. R. Stroberg, H. Hergert, J. D. Holt, S. K. Bogner, and A. Schwenk, *Phys. Rev. C* **93**, 051301 (2016).
- [18] A. Bohr and B. Mottelson, *Nuclear Structure* (W. A. Benjamin, New York, 1975), Vol. 2.
- [19] L. M. Polsky, C. H. Holbrow, and R. Middleton, *Phys. Rev.* **186**, 966 (1969).
- [20] A. Wuosmaa, J. Schiffer, B. Back, C. Lister, and K. Rehm, *Nucl. Instrum. Methods Phys. Res., Sect. A* **580**, 1290 (2007).
- [21] J. Lighthall *et al.*, *Nucl. Instrum. Methods Phys. Res., Sect. A* **622**, 97 (2010).
- [22] B. Harss *et al.*, *Rev. Sci. Instrum.* **71**, 380 (2000).
- [23] K. E. Rehm, J. P. Greene, B. Harss, D. Henderson, C. L. Jiang, R. C. Pardo, B. Zabransky, and M. Paul, *Nucl. Instrum. Methods Phys. Res., Sect. A* **647**, 3 (2011).
- [24] F. D. Becchetti, K. Ashktorab, J. A. Brown, J. W. Jänecke, D. A. Roberts, J. van Klinken, W. Z. Liu, J. J. Kolata, K. Lamkin, R. J. Smith, and R. E. Warner, *Phys. Rev. C* **42**, R801 (1990).
- [25] J. A. Brown, F. D. Becchetti, J. Jänecke, D. A. Roberts, D. W. Litzenberg, T. W. O'Donnell, R. E. Warner, N. A. Orr, and R. M. Ronningen, *Phys. Rev. C* **51**, 1312 (1995).
- [26] D. A. Roberts, F. D. Becchetti, J. A. Brown, J. Jänecke, K. Pham, T. W. O'Donnell, R. E. Warner, R. M. Ronningen, and H. W. Wilschut, *Nucl. Phys.* **A588**, c247 (1995).
- [27] D. A. Roberts, F. D. Becchetti, J. Jänecke, M. Y. Lee, T. W. O'Donnell, K. Pham, J. A. Brown, R. E. Warner, R. M. Ronningen, and H. W. Wilschut, *Phys. Rev. C* **65**, 044605 (2002).
- [28] J. A. Zimmerman *et al.*, *Nucl. Instrum. Methods Phys. Res., Sect. A* **579**, 476 (2007).
- [29] J. Lai *et al.*, *Nucl. Instrum. Methods Phys. Res., Sect. A* **890**, 119 (2018).
- [30] M. H. Macfarlane and S. C. Pieper, Argonne National Laboratory Report ANL-76-11, Rev. 1, 1978 (unpublished).
- [31] J. Testoni, S. Mayo, and P. Hodgson, *Nucl. Phys.* **50**, 479 (1964).
- [32] R. B. Wiringa, V. G. J. Stoks, and R. Schiavilla, *Phys. Rev. C* **51**, 38 (1995).
- [33] H. An and C. Cai, *Phys. Rev. C* **73**, 054605 (2006).
- [34] J. P. Schiffer, G. C. Morrison, R. H. Siemssen, and B. Zeidman, *Phys. Rev.* **164**, 1274 (1967).
- [35] R. L. Kozub, D. W. Bardayan, J. C. Batchelder, J. C. Blackmon, C. R. Brune, A. E. Champagne, J. A. Cizewski, U. Greife, C. J. Gross, C. C. Jewett, R. J. Livesay, Z. Ma, B. H. Moazen, C. D. Nesaraja, L. Sahin, J. P. Scott, D. Shapira, M. S. Smith, and J. S. Thomas, *Phys. Rev. C* **73**, 044307 (2006).
- [36] N. de Sereville *et al.*, *Nucl. Phys.* **A791**, 251 (2007).